Electronic Supplementary Material (ESI) for Catalysis Science & Technology.

Electronic Supplementary Information

Elucidating the effects of individual components in K_xMnO_y/SiO_2 and water on selectivity enhancement in the oxidative coupling of methane

Zeynep Aydin, Anna Zanina, Vita A. Kondratenko, Reinhard Eckelt, Stephan Bartling, Henrik Lund, Nils Rockstroh, Carsten R. Kreyenschulte, David Linke, Evgenii V. Kondratenko*

Leibniz Institut für Katalyse e.V. Albert-Einstein-Str. 29a, 18059 Rostock, Germany

* Corresponding Author: evgenii.kondratenko@catalysis.de; phone: +49(381)1281-290.

Table of content

Figure S7. (a,b) The overall rate of methane conversion and (c,d) selectivity to C_{2+} hydrocarbons over time on stream over (a,c) $4KMnO_4/SiO_2$ and (b,d) $16KMnO_4/SiO_2$ without (empty symbols) and with 30 vol% (filled symbols) water.

Figure S8. The selectivity to C_2H_6, C_2H_4, CO_2 and CO as function of methane conversion over $5K_2MnO_4/SiO_2$ at 800 °C without and with 30 vol% H_2O.

Figure S9. The selectivity to C_2H_6, C_2H_4, CO_2 and CO as function of methane conversion over $4KMnO_4/SiO_2$ and $16KMnO_4/SiO_2$ at 800 °C without and with 30 vol% H_2O.

Figure S10. The methane conversion rate into C_2, CO_2 and CO for the OCM reaction without (white bars) and with 30 vol% (black bars) co-fed H_2O over different catalysts at 800 °C in steady state.

Figure S11. Height-normalized transient responses of carbon-containing products after pulsing of (a-c) $^{18}O_2$:CH_4:He = 1:8:2 or (d-f) $^{18}O_2$:CH_4:H_2O:He = 1:8:0.85:2 mixtures at 800°C over different catalysts.

Mears Criterion for External Diffusion Limitations

To estimate the influence of external diffusion limitations, the Mears criterion was applied:

$$\frac{r_{obs} \cdot \rho_{catalyst} \cdot R \cdot n}{k_c \cdot C} < 0.15$$

r_{obs} – measured reaction rate, kmol/(kg_{cat}·s)

$\rho_{catalyst}$ – catalyst density, kg/m^3

R – catalyst pellet radius, m

n – reaction order

k_c – mass transfer coefficient, m/s

C – bulk concentration of reactant, kmol/m^3

For the OCM reaction at 800 °C over $10K_2MnO_4/SiO_2$ follows for the highest activity:

$\frac{r_{obs} \cdot \rho_{catalyst} \cdot R \cdot n}{k_c \cdot C}$ = [$5.67 \cdot 10^{-7}$ kmol/(kg_{cat}·s)]·[$1.12 \cdot 10^{3}$ kg/m^3]·[$2 \cdot 10^{-4}$ m]·2/([$1.90 \cdot 10^{-1}$ m/s]·[$4.49 \cdot 10^{-3}$ kmol/m^3]) = $\mathbf{2.99 \cdot 10^{-4} << 0.15}$

For the OCM reaction at 800 °C over $8KMnO_4/SiO_2$ follows for the highest activity:

$\frac{r_{obs} \cdot \rho_{catalyst} \cdot R \cdot n}{k_c \cdot C}$ = [$8.83 \cdot 10^{-6}$ kmol/(kg_{cat}·s)]·[$7.51 \cdot 10^{2}$ kg/m^3]·[$2 \cdot 10^{-4}$ m]·2/([$1.09 \cdot 10^{-1}$ m/s]·[$4.49 \cdot 10^{-3}$ kmol/m^3]) = $\mathbf{5.4 \cdot 10^{-3} << 0.15}$

Weisz-Prater criterion for Internal Diffusion Limitations

To estimate the influence of internal diffusion on the reaction rates, the Weisz-Prater criterion was applied:

$$\Psi = \frac{n+1}{2} \cdot \frac{r_{obs} \cdot \rho_{catalyst} \cdot R^2}{D \cdot C} \quad \text{(S1)}$$

If $\Psi < 1$, internal diffusion limitations are negligible.

n – reaction order

r_{obs} – measured reaction rate, kmol/(kg_{cat}·s)

$\rho_{catalyst}$ – catalyst density, kg/m^3

R – catalyst pellet radius, m

D – diffusion coefficient, m^2/s

C – bulk concentration of reactant, kmol/m^3

For the OCM reaction at 800 °C over $10K_2MnO_4/SiO_2$ follows for the highest activity:

Ψ = [(2 + 1)/2] [$5.67 \cdot 10^{-7}$ kmol/(kg$_{cat}$·s)]·[$1.12 \cdot 10^3$ kg/m^3]·[$(2 \cdot 10^{-4})^2$ m^2]/([$1.7 \cdot 10^{-4}$ m^2/s]·[$4.49 \cdot 10^{-3}$ kmol/m^3]) = $\mathbf{5.00 \cdot 10^{-5} < 1}$

For the OCM reaction at 800 °C over $8KMnO_4/SiO_2$ follows for the highest activity:

Ψ = [(2 + 1)/2] [$8.83 \cdot 10^{-6}$ kmol/(kg$_{cat}$·s)]·[$7.51 \cdot 10^2$ kg/m^3]·[$(2 \cdot 10^{-4})^2$ m^2]/([$1.7 \cdot 10^{-4}$ m^2/s]·[$4.49 \cdot 10^{-3}$ kmol/m^3]) = $\mathbf{5.22 \cdot 10^{-5} < 1}$

Mears Criterion for External Heat Transfer Limitations

The external heat transfer limitations were calculated as follows:

$$\frac{r_{obs} \cdot \rho_{catalyst} \cdot R \cdot E_a \cdot \Delta H}{k_g \cdot R_g \cdot T^2} < 0.15$$

r_{obs} – measured reaction rate, kmol/(kg$_{cat}$·s)

$\rho_{catalyst}$ – catalyst density, kg/m^3

R – catalyst pellet radius, m

E_a – activation energy, kJ/kmol

ΔH – reaction heat, kJ/mol

k_g – heat transport coefficient, kJ/(m^2·s·K)

R_g – gas constant, kJ/(mol·K)

T – reaction temperature, K

For the OCM reaction at 800 °C over $10K_2MnO_4/SiO_2$ follows for the highest activity:

$\frac{r_{obs} \cdot \rho_{catalyst} \cdot R \cdot E_a \cdot \Delta H}{k_g \cdot R_g \cdot T^2}$ = [$5.67 \cdot 10^{-7}$ kmol/(kg$_{cat}$·s)]·[$1.12 \cdot 10^3$ kg/m^3]·[$2 \cdot 10^{-4}$ m]·[$2.1 \cdot 10^5$ kJ/kmol]·[$8.09 \cdot 10^2$ kJ/mol]/([$1.38 \cdot 10^3$ kJ/(m^2·s·K)]·[$8.31 \cdot 10^{-3}$ kJ/(mol·K)]·[$(1.07 \cdot 10^3)^2$ K^2]) = $\mathbf{1.63 \cdot 10^{-6} < 0.15}$

For the OCM reaction at 800 °C over $10K_2MnO_4/SiO_2$ follows for the highest activity:

$\frac{r_{obs} \cdot \rho_{catalyst} \cdot R \cdot E_a \cdot \Delta H}{k_g \cdot R_g \cdot T^2}$ = [$8.83.67 \cdot 10^{-6}$ kmol/(kg$_{cat}$·s)]·[$7.51 \cdot 10^2$ kg/m^3]·[$2 \cdot 10^{-4}$ m]·[$1.2 \cdot 10^5$ kJ/kmol]·[$8.09 \cdot 10^2$ kJ/mol]/([$1.38 \cdot 10^3$ kJ/(m^2·s·K)]·[$8.31 \cdot 10^{-3}$ kJ/(mol·K)]·[$(1.07 \cdot 10^3)^2$ K^2]) = $\mathbf{2.51 \cdot 10^{-5} < 0.15}$

Table S1. BET surface area of K_yMnO_4/SiO_2 (y = 1 or 2) before and after OCM reaction without H_2O (1st dry cycle after 6 h) and with H_2O (in steady state after 120 h).

Catalysts	Specific surface area / m^2/g		
	before OCM reaction	**after OCM reaction without H_2O**	**after OCM reaction with H_2O**
$5K_2MnO_4/SiO_2$	2.92	1.59	0.36
$10K_2MnO_4/SiO_2$	0.87	0.09	0.06
$20K_2MnO_4/SiO_2$	0.19	0.10	0.15
$4KMnO_4/SiO_2$	8.95	5.09	0.51
$8KMnO_4/SiO_2$	5.34	3.18	0.36
$16KMnO_4/SiO_2$	4.22	1.33	0.38
SiO_2 (amorphous)	272.3		72.6
SiO_2 (α-cristobalite)	2.39		
$3Mn/SiO_2$	158.00		34.00
$5K_2O/SiO_2$	0.17		0.11
$3Mn\text{-}5K_2O/SiO_2$	0.63	0.47	0.20

Table S2. Near-surface composition (wt%) of K_yMnO_4/SiO_2 (y = 1 or 2) with different wt% of K_yMnO_4 (y = 1 or 2) before and after OCM reaction without H_2O (1st dry cycle after 6 h) and with H_2O (in steady state after 120 h) as determined by XPS. The corresponding bulk values determined by ICP-OES are given in the brackets.

Catalysts	Catalyst treatment	K	Mn	Si	O
$5K_2MnO_4/SiO_2$	Fresh sample	6.9 (1.8)	1.6 (1.4)	43.4	41.7
	After OCM without H_2O	6.6	1.7	44.6	42.5
	After OCM with H_2O	6.2 (1.8)	1.9 (1.4)	44.8	42.2
$20K_2MnO_4/SiO_2$	Fresh sample	14.6 (8.1)	3.8 (5.7)	36.6	37.7
	After OCM without H_2O	13.2	3.7	35.5	39.6
	After OCM with H_2O	13.3 (8.1)	3.9 (5.5)	37.9	38.7
$4KMnO_4/SiO_2$	Fresh sample	3.4 (1.1)	2.2 (1.5)	46.7	44.3
	After OCM without H_2O	5.0	4.0	43.6	43.7
	After OCM with H_2O	7.7 (1.0)	6.1 (1.3)	39.1	40.7
$16KMnO_4/SiO_2$	Fresh sample	5.7 (3.7)	2.6 (4.9)	44.0	44.3
	After OCM without H_2O	8.0	5.0	40.3	41.2
	After OCM with H_2O	7.7 (3.4)	6.5 (4.6)	38.9	41.8

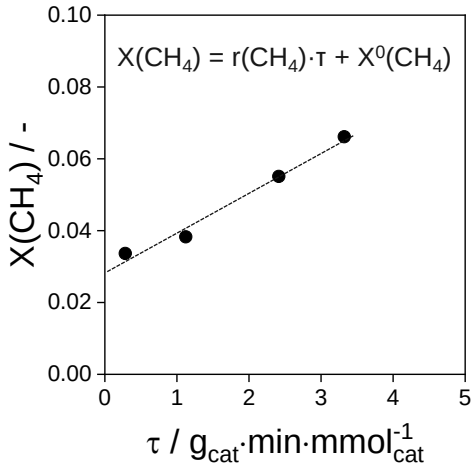

Figure S1. Determination of the methane conversion rate $r(CH_4)$ from the correlation between the methane conversion $X(CH_4)$ and the contact time τ.

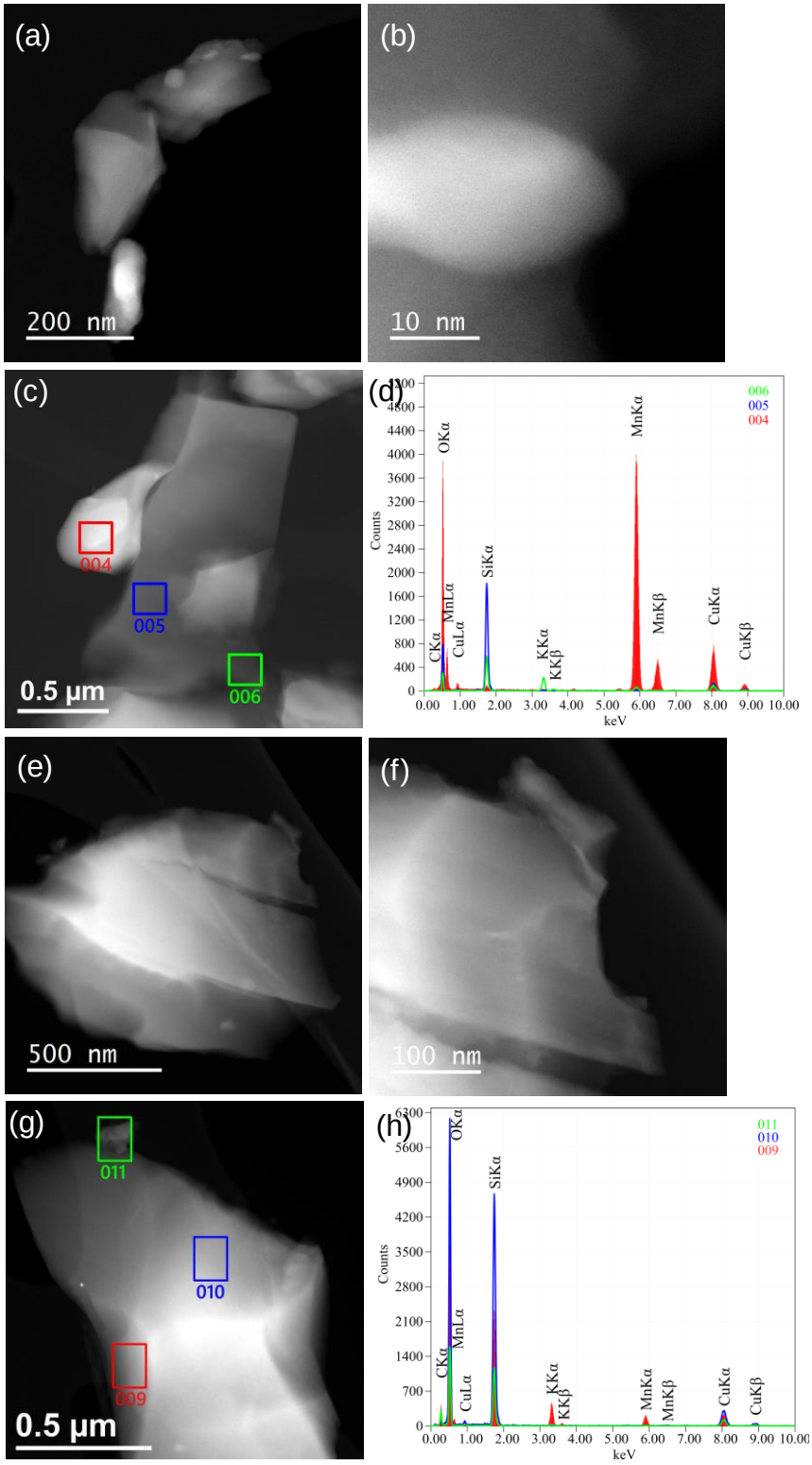

Figure S2. Representative STEM-HAADF images and EDX spectra of $10K_2MnO_4/SiO_2$ (a-d) before and (e-h) after OCM reaction with co-fed H_2O.

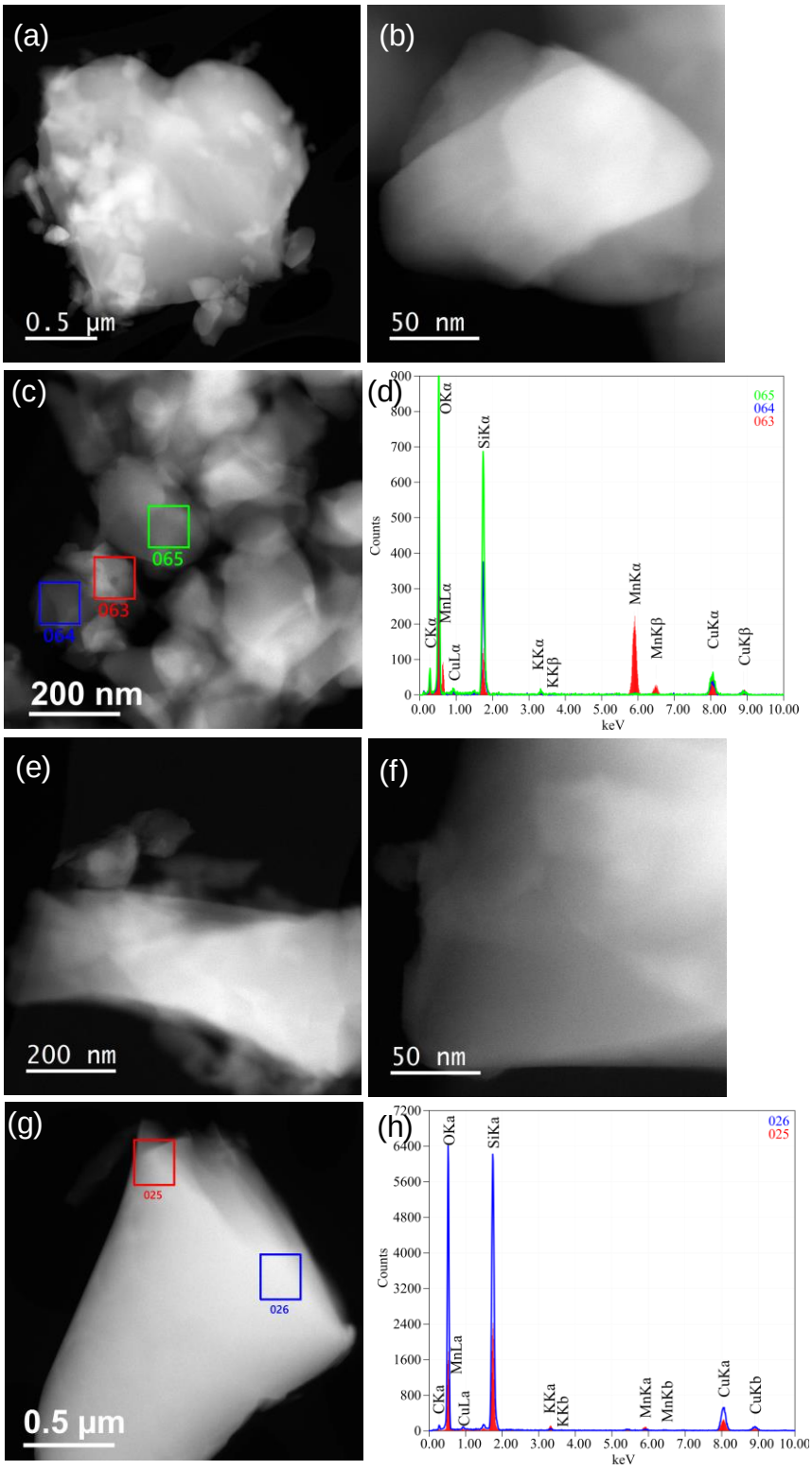

Figure S3. Representative STEM-HAADF images of $8KMnO_4/SiO_2$ and EDX spectra (a-d) before and (e-h) after OCM reaction with co-fed H_2O.

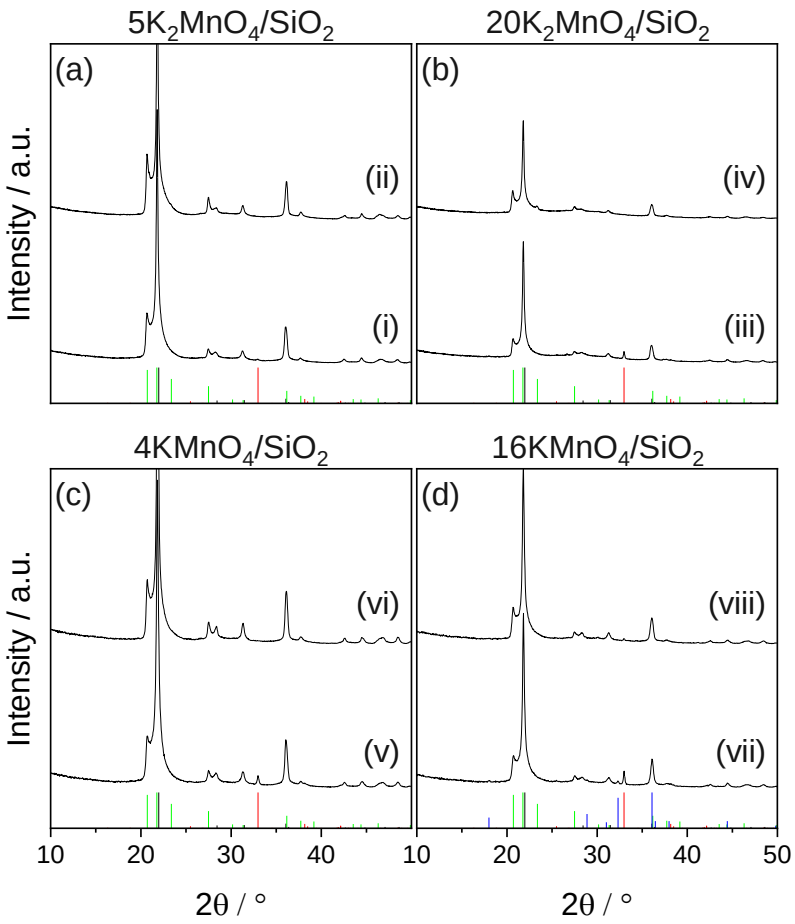

Figure S4. XRD patterns of (a) $5K_2MnO_4/SiO_2$, (b) $20K_2MnO_4/SiO_2$, (c) $4KMnO_4/SiO_2$ and (d) $16KMnO_4/SiO_2$ (i, iii, v, vii) before, (ii, iv, vi, viii) after OCM reaction with H_2O. $Mn_7O_8(SiO_4)$ (red bars) (PDF-No. 01-089-5662), Mn_3O_4 (blue bars) (PDF-No. 01-074-6605), tetragonal SiO_2 (black bars) (PDF-No. 01-074-9378) and orthorhombic SiO_2 (PDF-No. 00-042-1401) (green bars).

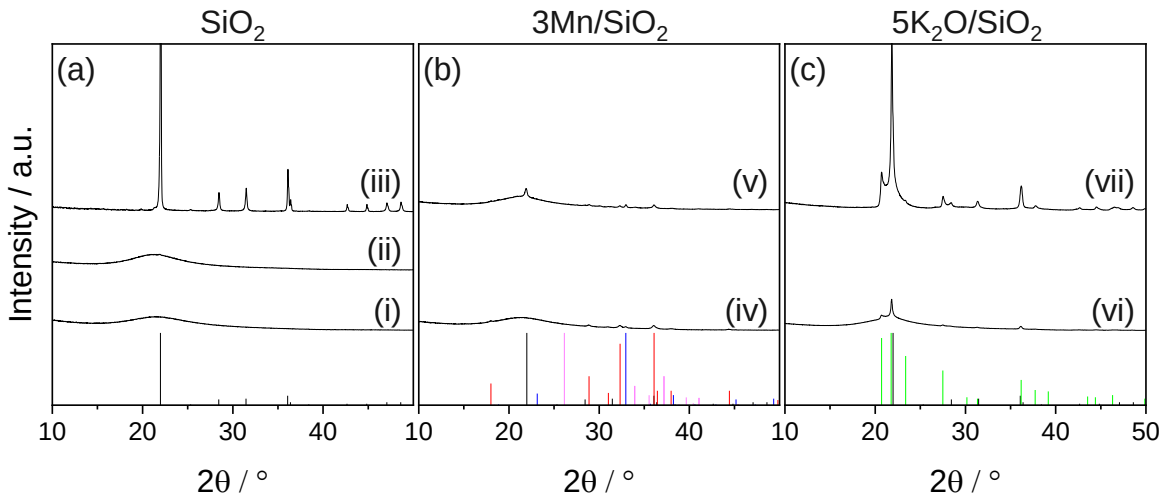

Figure S5. XRD patterns of (a) SiO_2, (b) $3Mn/SiO_2$ and (c) $5K_2O/SiO_2$ (i, iii, iv, vi) before, (ii, v, vii) after OCM reaction with H_2O. (iii) was calcined at 1600 °C, while all other samples were calcined at 800 °C. Tetragonal SiO_2 (black bars) (PDF-No. 01-074-9378), orthorhombic SiO_2 (PDF-No. 00-042-1401) (green bars), Mn_2O_3 (blue bars) (PDF-No. 00-041-1442), Mn_3O_4 (red bars) (PDF-No. 01-080-0382) and MnO(OH) (purple bars) (PDF-No. 01-088-0649).

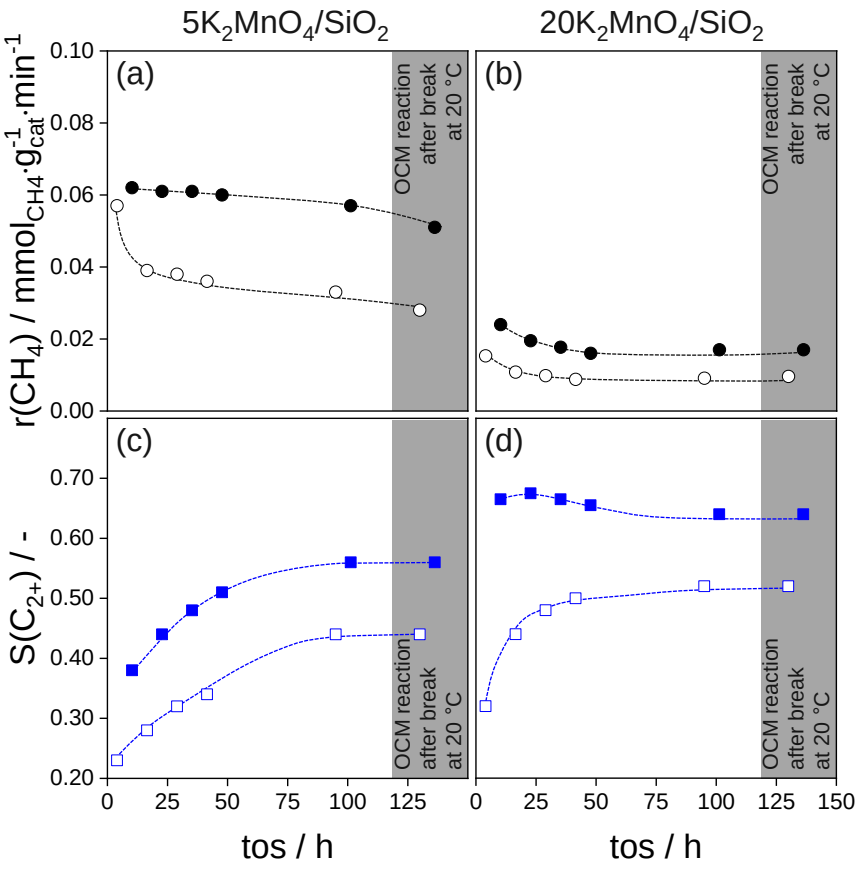

Figure S6. (a,b) The overall rate of methane conversion and (c,d) selectivity to C_{2+} hydrocarbons over time on stream over (a,c) $5K_2MnO_4/SiO_2$ and (b,d) $20K_2MnO_4/SiO_2$ without (empty symbols) and with 30 vol% (filled symbols) water; 800 °C, CH_4/O_2=8, 40 vol% CH_4, $X(CH_4)$ = 0.06, $0.3 \leq X(O_2) \leq 0.6$.

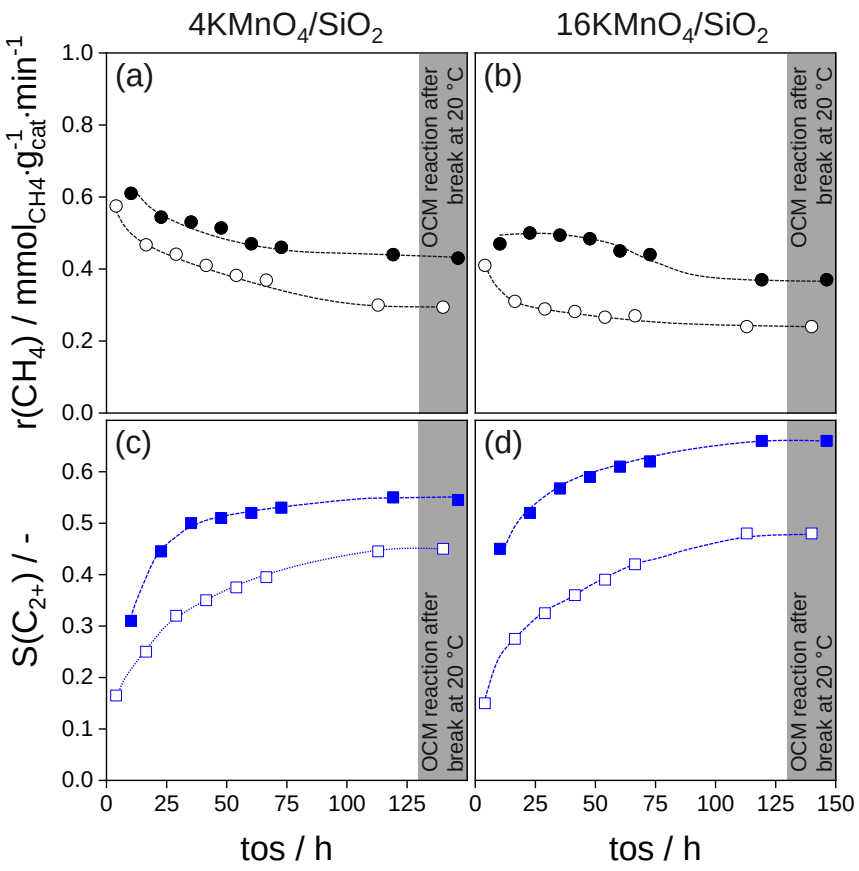

Figure S7. (a,b) The overall rate of methane conversion and (c,d) selectivity to C_{2+} hydrocarbons over time on stream over (a,c) $4KMnO_4/SiO_2$ and (b,d) $16KMnO_4/SiO_2$ without (empty symbols) and with 30 vol% (filled symbols) water; 800 °C, CH_4/O_2=8, 40 vol% CH_4, $X(CH_4)$ of 0.06, 0.3 $\leq X(O_2) \leq$ 0.6.

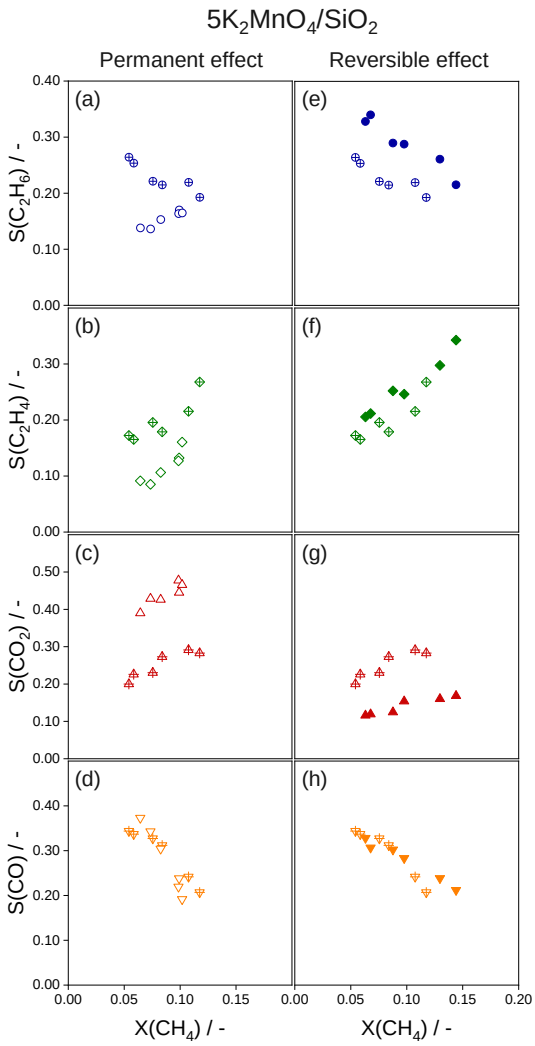

Figure S8. The selectivity to C_2H_6, C_2H_4, CO_2 and CO as function of methane conversion over $5K_2MnO_4/SiO_2$ at 800 °C without and with 30 vol% H_2O. (a-d) Permanent water effect is illustrated by comparison of the data under dry conditions from the 1st cycle (empty symbols) and 6th cycle (crossed symbols, after 114 h). (e-h) Reversible water effect is illustrated by the comparison of the data after 114 h under dry (crossed symbols) and after 120 h under wet (filled symbols) conditions; $0.4 \leq X(O_2) \leq 1.0$.

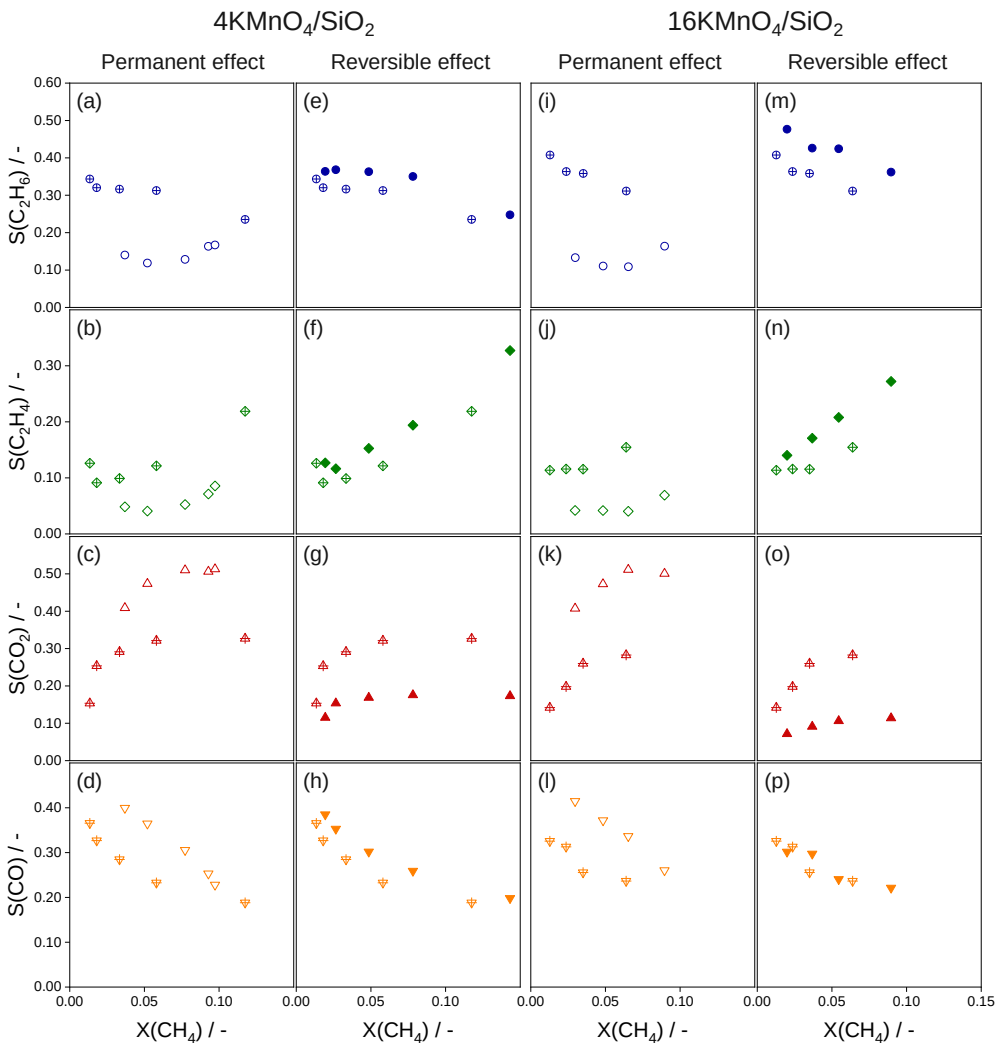

Figure S9. The selectivity to C_2H_6, C_2H_4, CO_2 and CO as function of methane conversion over $4KMnO_4/SiO_2$ and $16KMnO_4/SiO_2$ at 800 °C without and with 30 vol% H_2O. (a-d, i-l) Permanent water effect is illustrated by comparison of the data under dry conditions from the 1st cycle (empty symbols) and 6th cycle (crossed symbols, after 114 h). (e-h, m-p) Reversible water effect is illustrated by the comparison of the data after 114 h under dry (crossed symbols) and after 120 h under wet (filled symbols) conditions; $0.1 \leq X(O_2) \leq 1.0$.

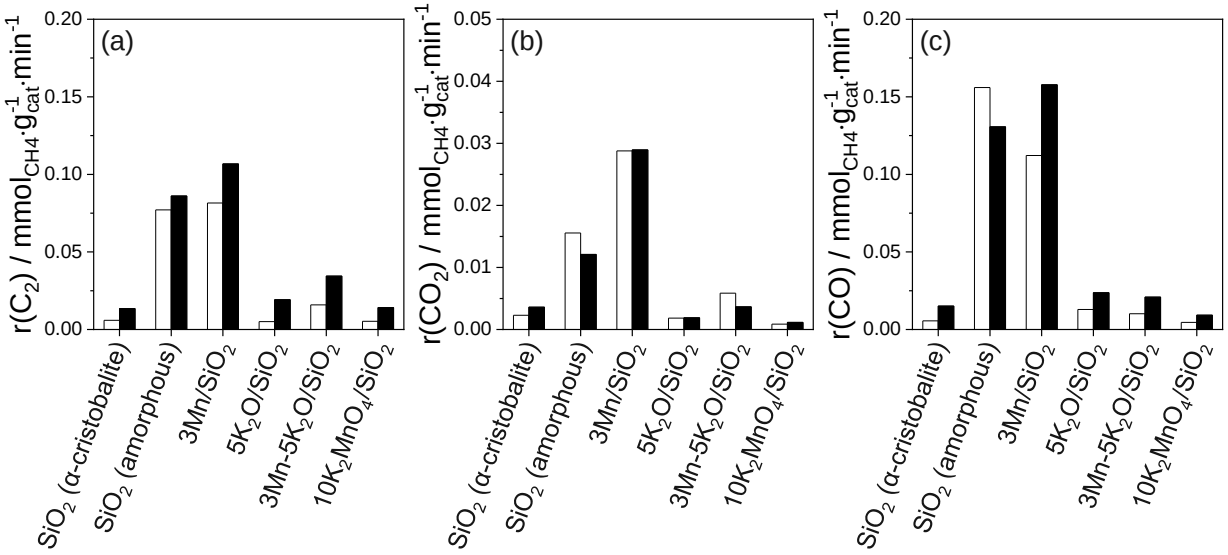

Figure S10. The methane conversion rate into C_2, CO_2 and CO for the OCM reaction without (white bars) and with 30 vol% (black bars) co-fed H_2O over different catalysts at 800 °C in steady state; $0.001 \leq X(CH_4) \leq 0.003$ for SiO_2 (α-cristobalite), $0.02 \leq X(CH_4) \leq 0.04$ for all other catalysts.

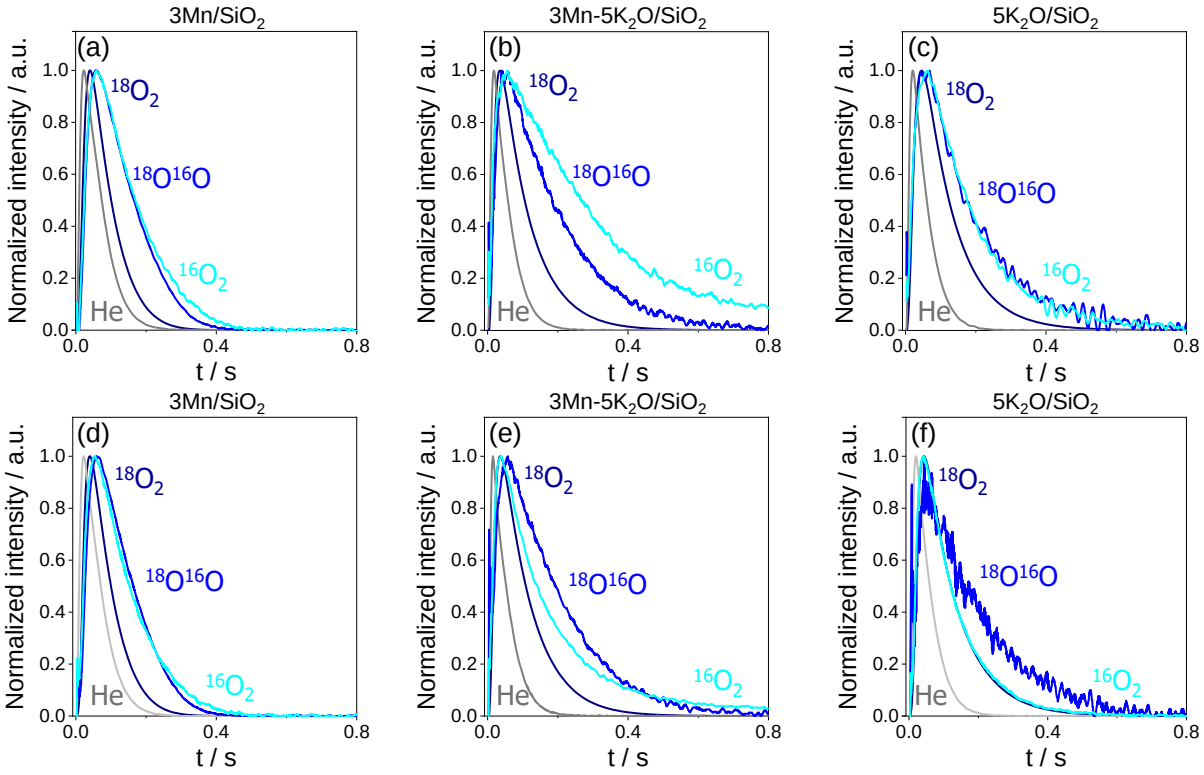

Figure S11. Height-normalized transient responses of carbon-containing products after pulsing of (a-c) $^{18}O_2$:CH_4:He = 1:8:2 or (d-f) $^{18}O_2$:CH_4:H_2O:He = 1:8:0.85:2 mixtures at 800°C over different catalysts.